6-2012

Carbon nanotube biosensors for detection of biomarkers in breast cancer cells.

Benjamin C. King
University of Louisville

CARBON NANOTUBE BIOSENSORS FOR DETECTION OF BIOMARKERS IN BREAST CANCER CELLS

By

Benjamin C. King
B.Sc., University of Louisville, 2009

A Thesis
Submitted to the Faculty of the
University of Louisville
J. B. Speed School of Engineering
as Partial Fulfillment of the Requirements
for the Professional Degree

MASTER OF ENGINEERING

Department of Bioengineering

June 2012

CARBON NANOTUBE BIOSENSORS FOR DETECTION OF BIOMARKERS IN BREAST CANCER CELLS

Submitted by: _____
Benjamin C. King

A Thesis Approved On

_____
(Date)

by the Following Reading and Examination Committee:

_____
Balaji Panchapakesan, Thesis Director

_____
Palaniappan Sethu

_____
Robert Cohn

ACKNOWLEDGEMENTS

Thanks to Dr. Baloo for his help and support throughout the project. Thanks as well to the Small Systems Lab members, James Loomis, Peng Xu, Hanwen Yuan, Michael Clark, and especially Tom Burkhead with whom I collaborated extensively on the device fabrication processes.

Tommy Roussel, Vanessa Velasco, Mark Crain, Joe Williams provided invaluable advice and instrument support. Numerous other researchers and staff at U of L provided valuable contributions as well.

I am grateful to my parents, David and Martha, for all their love and encouragement.

ABSTRACT

Detection and profiling of circulating tumor cells (CTCs) is useful for cancer screening and for managing treatment of carcinoma patients. Label-free technologies aim to accomplish detection rapidly with small, simple micro and nano devices. Carbon nanotubes are favorable molecular sensors due to their unique properties. They have been widely investigated for immunosensing of cancer biomarkers as free proteins, but very little has been done to detect biomarkers in intact cells and much remains to be understood regarding the mechanism of their sensing.

We have developed a simple carbon nanotube biosensor for epithelial cell adhesion molecule (EpCAM) for sensing EpCAM positive cells. Sensor fabrication steps involving minimal air exposure were employed which reduced random noise upon sample introduction to the device. Optimized sensors recognized specific interactions with EpCAM positive MCF-7 cells and did not recognize EpCAM negative MCF-10A cells, producing the same characteristic signal as for blank phosphate buffered saline samples (no interaction). A two sample *t*-test found that the specific and nonspecific signals were significantly different, $p = 0.0235$. Specific binding signals are attributed to the combined binding events and negative cell membrane potential.

.

TABLE OF CONTENTS

NOMENCLATURE

G	=	device conductance
V_G	=	gate voltage
V_{DS}	=	source-drain voltage
I_{DS}	=	source-drain current

LIST OF TABLES

LIST OF FIGURES

I. INTRODUCTION

Cancer is the second leading cause of death in the United States, totaling 567,628 deaths in 2009, the most recent complete data (Heart disease is the first with 599,413)[1]. Cancer cells originate from the body's own tissue and thus are difficult to distinguish from healthy cells, even undetectable by the body's own immune system. This presents a challenge for cancer diagnosis and therapy -- to identify malignant cells among normal ones, and to treat them with chemotherapeutics and other agents while preserving healthy tissue.

There are ways in which malignant cells belie their true nature however. They express certain surface markers, proteins embedded in the cellular membrane, at much higher levels than normal tissue. Much research has been done to identify these surface proteins, deemed cancer biomarkers, and correlate them to specific cancer types. To translate this knowledge into clinical utility, reliable and efficient testing methods are needed. Testing for cancer biomarkers can be used for cancer screening and for monitoring confirmed cancer cases.

Tumor biopsies are the most direct route to obtain samples for biomarker testing but their invasive nature is detrimental to the patient, and limits the number of tests which

can be done. Also for the purposes of screening, tumors must be detected by some other method before undergoing further tests.

Circulating tumor cells (CTC) are tumor cells which have escaped into the bloodstream and display the same biomarkers. CTCs were first documented in 1869 by Australian physician Thomas Ashworth, who identified cancer cells in the blood sample of a metastatic cancer patient by observing their morphology in a light microscope[2], [3]. Ashworth correctly predicted that CTCs were responsible for the spread of the cancer, but not until the recent identification of cancer biomarkers and development of molecular recognition technologies has their diagnostic potential been explored.

CTCs are present at concentrations of 50-300,000 cells/μL in metastatic cancer patients[4]. CTCs represent a less invasive sampling option and are systemic indicators rather than from one local tumor site [5]. The number of CTCs counted, and/or the biomarkers they display are strong indicators of patient prognosis[2], [6], [7], helpful in determining the efficacy of adjuvant therapies[4] and can even tell physicians whether certain treatments will be effective. For example Herceptin, a therapeutic agent which targets breast cancer biomarker Her2 antigen, is effective for Her2 + and ineffective for Her2 – cancers[8]. Taking cancer type into account, certain biomarkers indicate the patients prognosis and this information can be used to spare patients with positive prognoses from unnecessary chemotherapy[9].

In 2008, the Veridex CellSearch system became the first FDA approved method for CTC detection[10], [11]. The system takes a 7.5 mL blood sample and tags CTC with magnetic nanoparticles, and a fluorescent dye specific to epithelial cells. A magnetic field

pulls tagged cells to the surface of a sorting chamber. Then a fluorescent optical scan verifies which cells are CTCs and counts their number[2], [12]. The CellSearch system detects 85% of CTCs in a sample with 95% confidence, thus its detection limit is 1.2+/-0.4 CTCs per 7.5 mL sample[13]. The CellSearch technology is also being used as a research tool to gain new understanding of the metastatic process[14].

Its accuracy makes CellSearch a strong clinical tool but it is ultimately dependent on fluorescent molecular labeling and imaging in order to detect the CTCs. Therefore, it requires large sophisticated equipment. Likewise, the bulk of detection methods in current molecular biology practice utilize a labeling step and subsequent optical imaging step to detect target molecules. The label is a molecule, tagged with a dye or other indicator, which specifically binds to a target molecule. Antibodies, aptamers, complementary DNA and other molecules can be used to bind specifically to targets. Fluorescent dyes, enzymes, quantum dots, and other indicators can all be used as tags[15]. These labeling schemes typically require extensive sample preparation and sophisticated optical imaging devices.

Label-free techniques are being developed in an attempt to achieve the high accuracy of standard molecular labeling at lower cost and complexity, thus improving the accessibility of biomolecular information. This enables doctors to more effectively treat their patients in the clinic, and researchers to acquire more complete knowledge in the laboratory.

Label-free detection typically requires biomolecular interactions to be transduced into electrical or mechanical signals. Carbon nanotubes are ideal biomolecular

transduction elements. Many properties of single-wall carbon nanotubes (SWNT) make them desirable for these applications. Consisting of just a single carbon layer, their diameter (~1 nm) is on the same order of size as many biomolecules, and every atom is on the surface, exposed to the surrounding environment. They can be several microns or even on the order of centimeters in length, which permits them to transmit signals over relatively large distances.

Antibodies specific to cancer biomarkers, or other molecules of interest, can be conjugated to the carbon nanotube sidewalls. Specific binding of the target molecule to these conjugated antibodies alters the electrical response of the carbon nanotube, presumably due to charge transfer and capacitive coupling. This can be readily observed and has been demonstrated for free proteins, DNA, metabolites and others, but reports of cellular sensing with these devices have not yet emerged in great number.

The promise of biosensing with carbon nanotubes entails low cost devices which can rapidly detect multiple biomarkers via electrical signals, without the need for complex equipment and procedures. Our present challenge is to understand and characterize the electrical signals for immunosensing of cancer biomarkers on intact cells. Contained in this thesis is a description of unique specific signatures for MCF7 mammary adenocarcinoma cells which overexpress EpCAM.

II. BACKGROUND

A. Epithelial Cell Adhesion Molecule, Cancer Biomarker

Specific recognition of Epithelial Cell Adhesion Molecule (EpCAM) in epithelial cells is the focus of this study. EpCAM was chosen as a model system because it is present in nearly all adenocarcinomas and squamous cell carcinomas[16]. In fact it is so ubiquitously present in CTCs that the aforementioned CellSearch system exclusively uses anti-EpCAM-magnetic nanoparticle conjugates to sort CTCs from blood samples[13].

EpCAM was first identified by the production of an antibody, designated 17-1A, from mice immunized with human colorectal carcinoma derived cells[17]. 17-1A was found to bind specifically to colorectal carcinoma cells, but not normal colon tissue, nor to other malignant cell types such as melanomas, astrocytomas and fibrosarcomas.

EpCAM functions in mediating homophilic cell-cell adhesion, hence its name. EpCAM is a 314 amino-acid tetrameric polypeptide with a 242 amino-acid extracellular domain. It is only present in epithelial cells. The extracellular domain contains epidermal-growth-factor-like domain and a thyroglobulin (TY) domain. A 26 amino acid cytoplasmic domain associates with the actin filaments of the cytoskeleton[16].

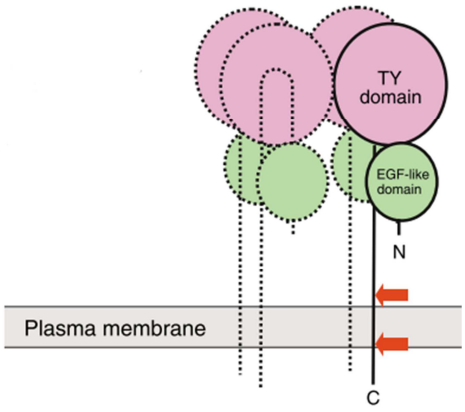

Figure II.1 Revised EpCAM structural model, from [16]

EpCAM's role in cancer is a complicated one. By forming cell-cell adhesions, EpCAM inhibits metastasis when transfected into tumor cells in mice. However EpCAM adhesions are weaker than common cell-cell adhesions such as cadherins, and increased EpCAM expression is correlated with decreased cadherin expression. So by replacing strong cell-cell adhesions with weaker ones, EpCAM could facilitate metastasis. Thus for some cancers (breast, ovarian and others) EpCAM expression has a negative influence on patient survival, but for other cancers (gastric, renal and others) EpCAM expression has a positive influence on patient survival[16], [18]. The 17-1A antibody was investigated as a therapeutic agent itself and adjuvant therapy of colorectal cancer patients successfully reduced their 7 year mortality, but it was ineffective against large solid tumors[18].

In either case, EpCAM expression correlates with increased proliferation and de-differentiation of cells. EpCAM mediates a signaling pathway which can be triggered through zones of cell-cell contact. When triggered, EpCAM is cleaved by proteases and an intracellular peptide termed EpIC is released. Intracellular receptors for EpIC initiate

the formation of a multiprotein signaling complex which has shown to be involved in growth promoting effects[16].

EpCAM makes an ideal model system due to its ubiquity in carcinomas and CTCs, apparent signaling role, and prognosis indication.

B. Clinical Relevance of CTCs

CTCs are present in the bloodstream of patients with malignant epithelial tumors at 50-300,000 cells/mL[4], but are quite rare compared to the number of mononuclear cells in the same volume, only one per million or 10 million[9]. Early stage cancers are expected to have far fewer CTCs, so detection of CTCs is very much a needle-in-the-haystack type problem. Furthermore, due to the heterogeneous nature typical of malignant tumors, cancer types do not always display the same biomarkers. Cells from within the same tumor may not even display the same biomarker profile, thus there is still disagreement over the proper CTC testing methods and interpretation of the results[19], [20].

Because they are rare events, enrichment protocols can be employed to increase the concentration of CTCs, but at the risk of sample loss during the enrichment[20]. Micro and nanotechnologies are under development to provide CTC enrichment with low sample loss[21–26]. It is likely that micro and nanotechnology applications in this area will advance alongside detection applications.

C. Molecular Recognition

Specific molecular interactions are necessary for the elaborate organization of our bodies. Cells display surface markers and receptors with precisely defined structures that contain recognition sequences. Complementary sequences exist on other molecules, such as growth factors or markers displayed on other cells, which are only complementary to that molecule and may bind specifically to it with a force proportional to the change in enthalpy, minimizing the free energy[27]. Binding events can and usually do set off signaling cascades, enabling cells to interact with each other and the environment.

Biology has taken advantage of specific binding to investigate the properties and behaviors of cells. Antibodies are raised to form a complementary sequence which binds specifically to a region of a desired target molecule. Researchers can use antibodies tagged with a dye, enzyme or other signal molecule to determine the presence of a molecule of interest in cell, tissue or other samples. This sums up labeled detection.

Label-free detection attempts to circumvent the label by measuring intrinsic properties of the binding event itself. This is where micro and nanotechnology come into play. Structures fabricated on a nanometer or micrometer length scale are sensitive to forces and signals in delicate biological systems which could never be observed at the macroscale.

Stresses due to free energy change upon specific binding have been investigated with microcantilever arrays [28–31]. One half of the binding pair, i.e. an ssDNA or receptor, is attached to the surface of the microcantilever. When the complementary ssDNA or ligand is introduced, the specific binding generates an expansive stress on the

cantilever surface causing it to deflect. The microcantilevers must be very soft to respond to this small force, thus there is considerable cantilever motion due to the movement of the fluid. Precise position measurement relative to a reference (unfunctionalized) cantilever is required to detect the deflection due to binding which somewhat offsets the label-free advantage of these sensors. Nonetheless, the microcantilever deflection illustrates the power of nanotechnology to resolve biomolecular binding events.

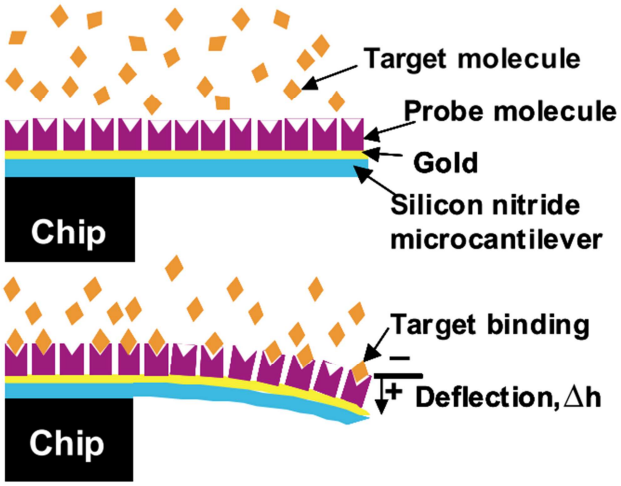

Figure II.2 Specific binding causes microcantilever deflection, from [29]**.**

D. Carbon Nanotube Biosensors

Electrical sensing offers a more streamlined approach than measuring sub-nm mechanical deflections. Carbon nanotubes, along with nanowires and recently graphene [32] have been investigated as transduction elements for biosensing. Nanowires perform reliably but their high resistance limits their resolution. Carbon nanotubes have much lower resistance and are ideal transduction elements but variations in as-prepared

nanotube products and their network behaviors have limited their ultimate sensing performance.

1. Carbon Nanotube Properties

Multi wall carbon nanotubes were discovered in 1991 [33], single wall carbon nanotubes in 1993 [34]. With reports of their extraordinary electrical and mechanical properties [35], biosensing applications for carbon nanotubes soon fell under investigation. Single wall carbon nanotubes (SWNT) are one dimensional molecular wires. They are capable of ballistic electron transport along their axis, with micron order mean free paths. They can be metallic or semiconducting. Nanotube synthesis typically produces a 1:2 metallic:semiconducting ratio. This transport property is dependent on the angle of the carbon lattice with respect to the tube axis[36]. The semiconducting fraction of SWNTs are p-type semiconductors. As such, holes are the primary charge carriers and a negative gate voltage switches them on. They are also sensitive to mechanical strains, tension attenuates their conductance[37].

Despite advances in the processing, manipulation, and orienting of carbon nanotubes, it is not yet feasible to place continuous nanotubes in parallel between terminals over extended distances (10s or 100s of μm). Covering areas of this scale requires an interconnected carbon nanotube network. Conduction pathways are made up of several nanotubes each (some semiconducting and some metallic). Resistance between SWNTs in junctions of the networks are much higher than the resistance along the tube axes and contribute significantly to the resistance of the thin film.

2. *Functionalization*

A necessary first step for biosensor development is the attachment of biomolecules to the nanotube sidewalls. Reports of this emerged as early as 1999 when streptavidin proteins were shown forming helical crystals around multi wall carbon nanotubes[38]. Likewise antibodies and other targeting proteins nonspecifically adsorb onto nanotube sidewalls, but tend to adsorb nonspecifically to surrounding surfaces as well.

The use of linker molecules was developed to attain higher specificity of the proteins for the nanotubes during the conjugation process. Molecules such as pyrenebutanoic acids[39], streptavidin-biotin complex, and G proteins[40] have been used to attach the antibodies to the nanotube sidewalls with more uniform orientation.

Further chemical functionalization after the antibody attachment is useful to block any unoccupied nanotube sidewall areas. Sensors may be incubated in a detergent such as Tween20, TritonX, sodium dodecyl sulfate and others. The hydrophobic region of the detergent adsorbs onto the nanotube sidewall while the hydrophilic end repels proteins away. This minimizes the contribution of nonspecific interactions to the signal.

3. *Sensing mechanisms*

Carbon nanotube biosensors have been designed to detect DNA[41–45], glucose[43], [45–47], enzymes[45], [48], [49], protein-ligand interactions[50], and cancer biomarkers[51–55]. Regarding cancer biomarkers, carbon nanotube biosensors have, to this point, mainly been developed for free proteins whose elevated levels in blood serum

also indicate cancer. Prostate specific antigen (PSA) is a model system for this type of detection. Detection limits of these sensors and others are shown in Table II.1.

Table II.1 Comparison of selected biosensors

Sensor type	Target	Detection Limit	Sample Volume
Microcantilever	ssDNA	40 ng/mL (3μM) [30]	100 μL
	PSA	0.2 ng/mL [29]	-
Aligned CNT Thin Film, Quartz substrate	PSA	100 pM [51]	-
CNT Thin Film	PSA	1 ng/mL [52]	5.0 μL
	IgG	1 pg/mL [53]	10 μL
Magnetic Nanosensor	EpCAM	1 pM [56]	100 μm^2

Typical electrical measurements from the biosensors are given as device conductance (G) plotted vs. time and normalized to the initial device conductance (G_0). A class of CNT thin film biosensors utilize the Schottky barrier formed at the nanotube-metal contact for biosensing [57], [58], but the devices in this work have insulated electrodes which should avoid the Schottky barrier effects.

The prevalent sensing mechanism described for CNT biosensors is the gating effect of the target proteins as they bind to the antibodies. Binding of the targets to the antibodies brings them near the CNT [58], [59], within the debye length of the fluid. Positively charged proteins switch off semiconducting p-type CNT, decreasing device conductance [51], [53], [60], [61]. Negatively charged proteins switch on the CNTs,

increasing the conductance [52]. Also, for n-type semiconducting nanowires, positively charged proteins were shown to switch them on and increase conductance [61].

Reports of free EpCAM detection by CNT biosensors have not been found in the literature, but EpCAM detection was included in a multiplexed magnetic nanosensor [56] (included in Table II.1).

Human cells present a more complicated target than a protein, DNA, or other biomolecule whose charge is a function of the solution pH. The cell surface contains transport channels which pump ions in and out of the cell to maintain a membrane potential. For epithelial cells, the membrane potential is typically 10-50 mV. There are also many other surface markers present, aside from the specifice target, EpCAM, which could interfere with the specific antibody-antigen interactions.

Electrical identification of cells by their specific binding to their surface markers is also relatively unexplored. A prominent paper by Ning Shao *et al.* [54] is one of the few to report specific electrical detection of epithelial cells by antibody-conjugated carbon nanotubes. Sensors were constructed with just a few SWNT spanning a small 1 μm gap. Antibodies for breast cancer biomarkers Her2 or IGF1R were attached to the nanotubes via a 1 pyrenebutanoic acid, succinimidyl ester linker molecule. The devices were exposed to an excess of breast cancer cells, lines MCF7 and BT474 which overexpress IGF1R and Her2 respectively. For specific pairings, the normalized conductance, G/G_0 dropped to ~0.2. The attenuation was attributed to tensional and torsional strain generated by specific binding. The nanotubes were immobilized on each end by the electrodes, and specific binding of the cell strained the nanotubes against the

immobilization points. The authors predicted that similar effects would not be observed in an interconnected network (thin film) where nanotubes were not immobilized, but free to move independently.

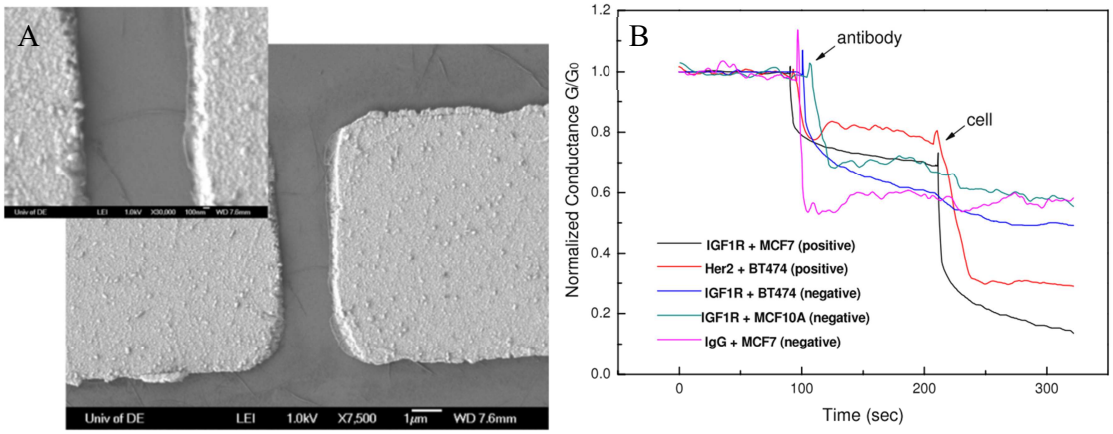

Figure II.3 (A)SWNT span 1 μm electrode gap, and (B) conductance attenuation for specific binding, from [54]**.**

Unfortunately, larger area sensors will be needed to detect cancer cells at clinically relevant concentrations and sample volumes. The goal of this study was to develop a thin film CNT biosensor capable of detecting EpCAM surface markers in cells. The remainder of this thesis covers the steps taken to achieve this goal. EpCAM (MCF-7) positive and EpCAM negative (MCF-10A) cell lines were cultured. Sensors were designed and fabricated, using thin films tailored to improve sensing performance. Antibody functionalization and testing protocols were designed to minimize signal disturbances. EpCAM positive (MCF-7) and EpCAM negative (MCF-10A) cell lines were tested with the sensor and distinct signals for the two lines were analyzed and discussed.

III. METHODS

A. Cell Culture

The MCF-7 cell line was used to simulate a circulating tumor cell. MCF-7 is a breast adenocarcinoma line which overexpresses EpCAM. The MCF-10A cell line was used as a control for the experiment. MCF-10A is a non-tumorigenic breast epithelial line with no EpCAM expression [62]. Cryogenically frozen vials of both cell lines were obtained from ATCC (item numbers HTB-22 and CRL-10317 for MCF-7 and MCF-10A respectively).

Culture media for MCF7 was EMEM (ATCC #30-2003) with 10% fetal bovine serum (FBS) (Cellgro #35-010-CV), 0.01 mg/mL human recombinant insulin (Sigma #I9278), and 10 nM β-estradiol (Sigma #E2758). Culture media for MCF-10A was MEBM (Lonza #CC-3150), minus the included GA-1000 growth supplement, plus 100 ng/mL cholera toxin (Sigma #C8052).

Confocal microscopy was used to confirm that EpCAM was present on MCF7 and absent on MCF-10A. Cells were grown on class coverslips, then fixed in formaldehyde for 20 minutes. They were stained with primary antibody solution (2 μg/mL, mouse monoclonal anti-EpCAM, EMD #OP187) for 30 minutes at 37°C, then

stained in secondary antibody (1:250 dilution of Dylight 488 conjugated goat-anti-mouse, Abcam #ab986789). Finally a DAPI nucleus stain was applied for 5 minutes at room temperature. Coverslips were rinsed again and mounted on glass slides with SlowFade Gold reagent.

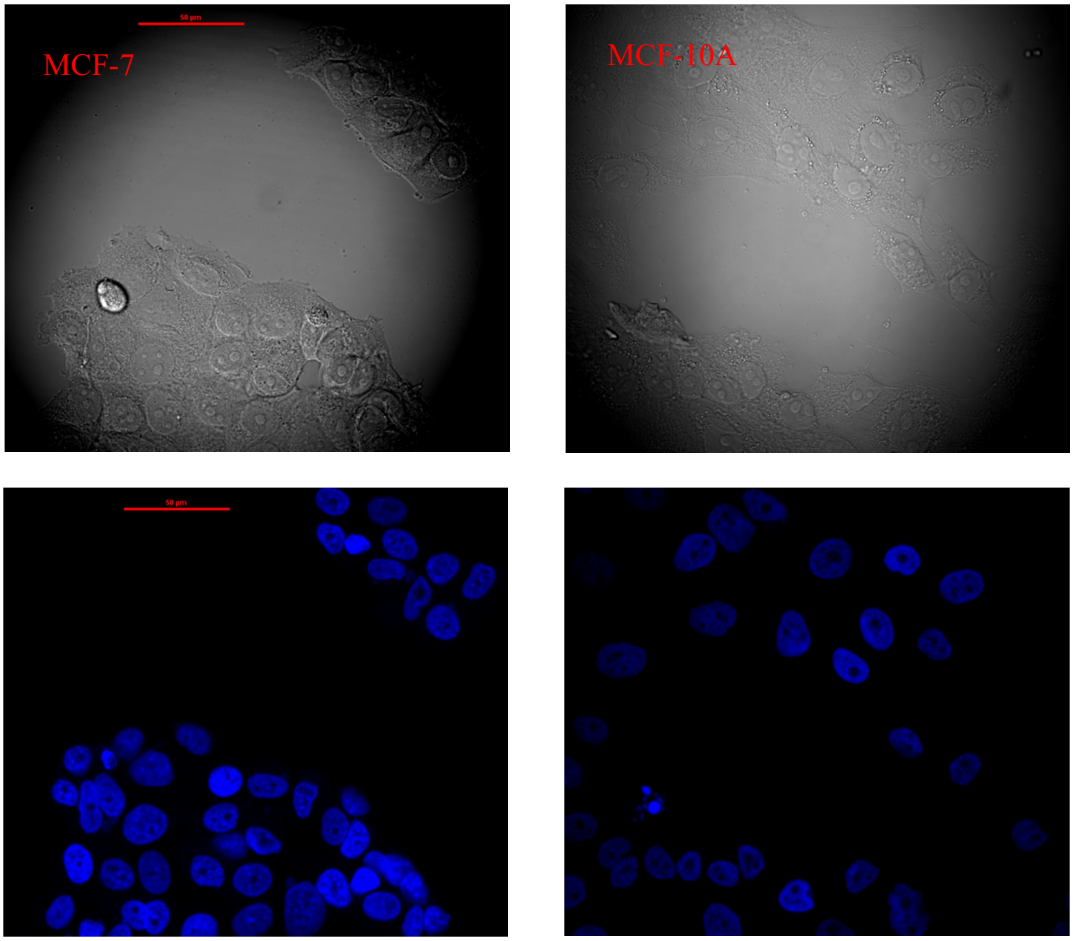

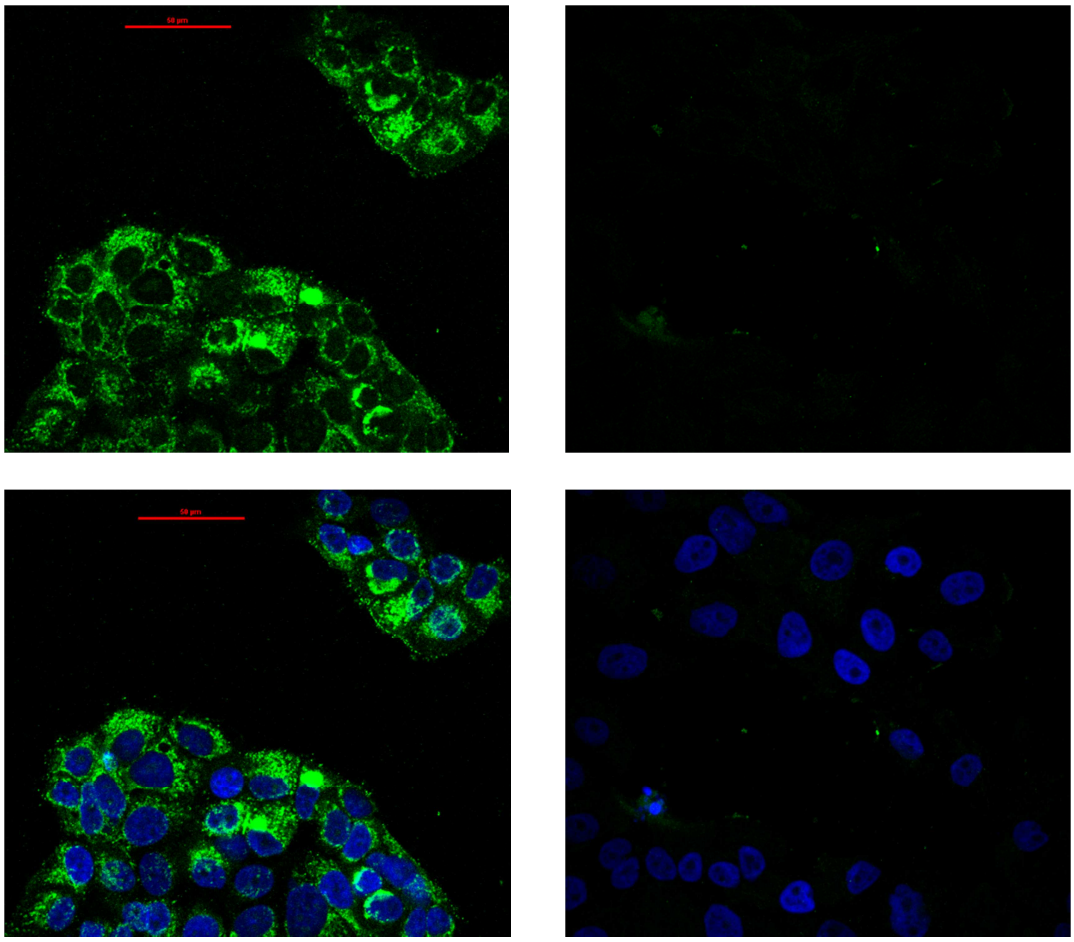

Figure III.1 Confocal microscopy of MCF7 (left) and MCF10A (right) cell lines. Green channel is anti-EpCAM stain. 60x magnification, 50 µm scale bar.

For testing, cells were grown to high confluency, then detached using Accutase solution (Sigma #A6964). Accutase was used in lieu of trypsin in an attempt to preserve the surface markers on the cells so that the antibodies functionalized onto the device could specifically recognize them. The cells were then centrifuged for 5 minutes at 220 g and resuspended in PBS at 10,000 cells/µL. Cells suspended at this high concentration were directly pipetted onto the devices to conduct the tests.

Jurkat E6-1 cells (purchased from ATCC, #TIB-152), CD4+ lymphoblasts, were also used as control samples. They were cultured in RPMI-1640 media (ATCC #30-2001) supplemented with 10% FBS (Cellgro #35-010-CV).

B. Carbon Nanotube Sensor Fabrication

The sensors are a simple two-terminal design. A carbon nanotube network connects two Cr/Au electrodes and the electrodes are covered by an insulating layer of SU8 photopolymer.

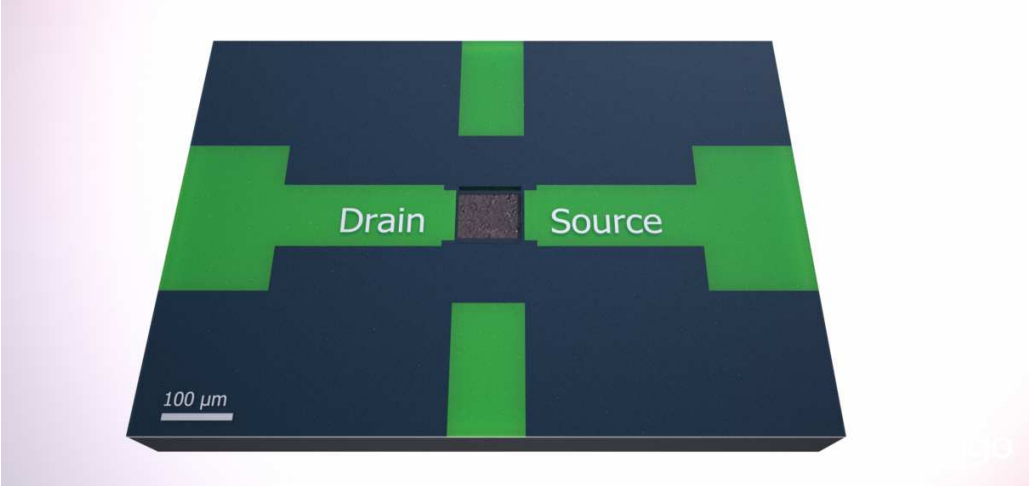

Figure III.2 Top down view of sensor showing SWNT thin film element and SU8 insulating layer

The first step in the process is assembling the nanotube network. A 99% weight, CCVD synthesized, single wall/double wall carbon nanotube mixture was purchased from Cheap Tubes Inc. Nanotubes are listed at 1-2 nm outer diameter and 3-30 µm length. Nanotubes were suspended in IPA at 45 µg/mL and sonicated for 90 min. The

solution was then diluted to 3.5 µg/mL and sonicated for 3 hours to completely disperse the nanotubes.

15 mL of the suspension was then further diluted with 85 mL of IPA before vacuum filtration over a cellulose membrane, 0.22 µm pore size. This method self-regulates the deposition rate of nanotubes on the membrane to produce an evenly distributed network [63]. The network is then pressed onto an oxidized (400 nm thickness) silicon wafer for 30 minutes. Next the wafer is transferred to an acetone vapor bath which dissolves the membrane.

The targeted thin film density was <5 CNT/µm, while still producing stable and reproducible devices. Very thin films exposed more nanotube sidewalls and reduced the number of junctions per nanotube so that nanotube resistance was more significant relative to the junction resistance. Both of these attributes improved the sensing properties of the film. SEM images were surveyed to determine the film density (Figure III.3). Counting nanotube intersections with a grid of 1 µm lines superimposed on the image yielded a mean density of 3.93 CNT/µm. The distribution of the nanotubes was favorable as well. The standard deviation was 3.22, therefore over 68% of the film area is favorable for sensing, containing 1-8 CNT/µm. See appendix for additional distribution data.

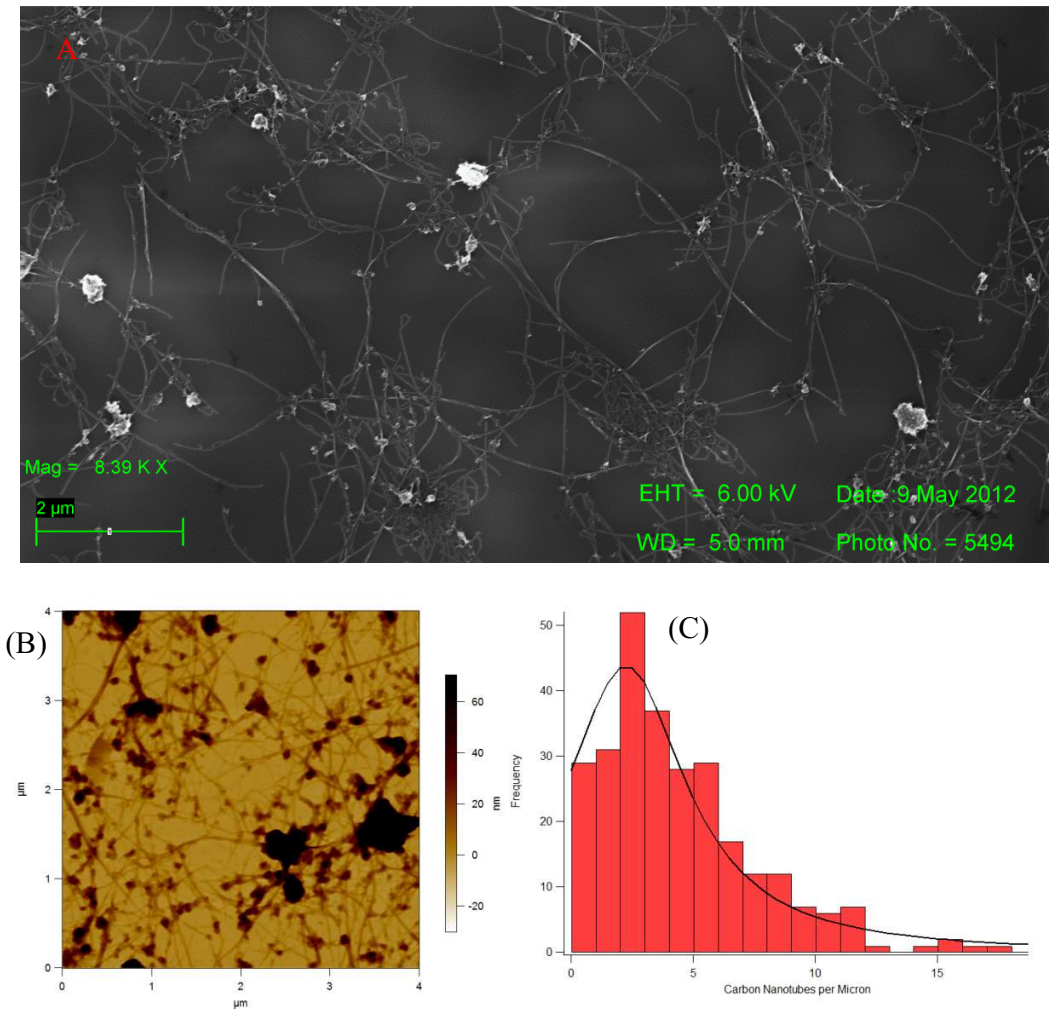

Figure III.3 Carbon nanotube thin film characterization. (a, previous page) SEM image. (b) AFM topography image. (c) Histogram of thin film density obtained by counting the number of nanotubes intersecting each element in an array of 1 µm lines superimposed on the SEM image in (a).

Patterning of the nanotube film and electrode and insulating layer fabrication are done by photolithography in the cleanroom. Photomasks for these steps were designed by Ms. Vanessa Velasco. AZ4620 photoresist is used to mask the nanotube film areas needed for the sensor elements. Exposed nanotubes are etched away in a March reactive ion etcher for 90 s at 200 W power and 10% O_2. SC1827 photoresist is used to mask the

electrode pattern. Electrodes consist of a 10 nm Ni adhesion layer and a 90 nm Au layer. They are deposited by sputtering in a Leskar PVD 75 system, 300 W DC power. Lastly, the sensors are covered with SU8-2005, a 5 μm thick photopolymer layer. A window over each of the nanotube sensor elements is developed but the electrodes remain insulated beneath the SU8.

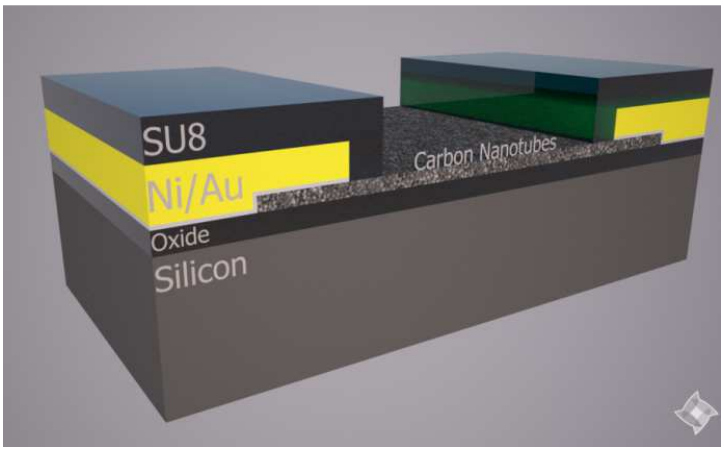

Figure III.4 Cut-away view of the device, not to scale.

C. Carbon Nanotube Functionalization

Finished carbon nanotube sensors were functionalized with anti-EpCAM by a pyrene linker molecule. The pyrene rings of 1-Pyrenebutanoic acid, succinimidyl ester (PASE) adsorb onto carbon nanotube sidewalls by π-stacking. The ester on the other end of the molecule provides an attachment point for antibodies. PASE (AnaSpec, #81238) was dissolved in methanol at 1 mg/mL. Devices were incubated in the PASE solution for 1 hour at room temperature, then rinsed with methanol and water. Devices were then incubated in anti-EpCAM (10 μg/mL in PBS, EMD Bioscience, #OP187) for 1 hour at 37°C. Lastly, a surfactant, Tween20, was used to block unfunctionalized nanotube

sidewalls or PASE sites in order to minimize nonspecific interactions. Devices were incubated in 0.5% Tween20 for 2 hours at room temperature. After incubation, devices were washed with water, then each incubated in a 2 µL droplet of PBS overnight in a humid chamber before testing.

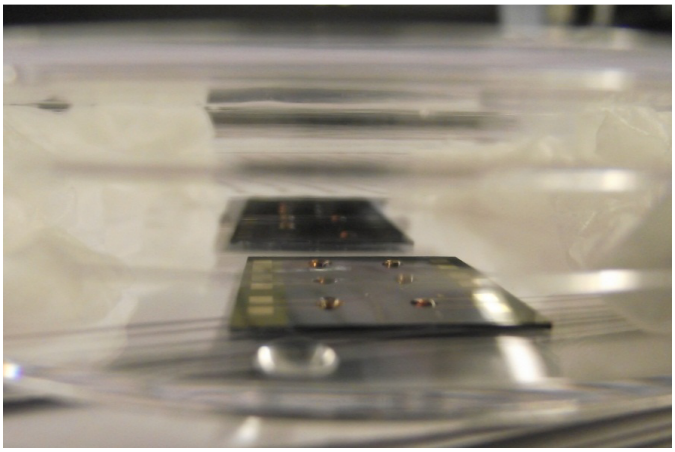

Figure III.5 Sensors, 6 per chip, incubating in Tween20 droplets in a humid chamber.

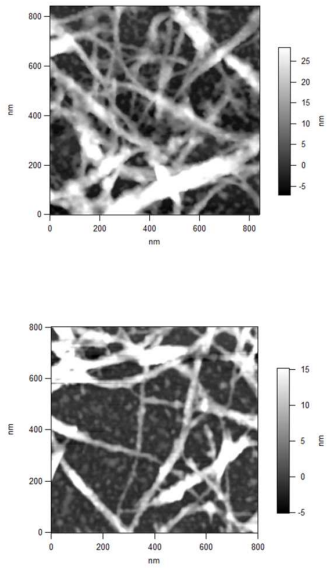

Figure III.6 PASE-mab functionalized nanotube film (top) and bare film (bottom). Minimum measured height is 5nm for the functionalized film and 3nm for the bare film.

D. Testing Protocol

The exact test protocol was revised throughout the course of the study as more was learned about the characteristics of the sensors, but the instrumentation set-up and many parameters remained constant.

Devices were placed on a Signatone probe station and the probe tips contacted the device at the source and drain terminals (Figure III.7). These were wired to an Agilent 4156C Semiconductor Parameter Analyzer which was controlled via a custom LabVIEW interface, developed by Mr. Tommy Roussel, running on a windows PC. A 100 mV bias was applied and the source drain current, I_{SD}, was recorded for the duration of the test.

Test solutions and samples were pipetted directly onto the device. In some cases the test was initiated with the device already hydrated and samples were pipetted into this droplet. The final testing protocol started with the device hydrated in a 2 µL droplet which was placed immediately after functionalization and left overnight. The bias was applied, and then a 5 µL droplet, either of cell suspension, PBS or water, was pipetted directly into the standing 2 µL droplet. To compare results among devices, I_{SD} data were normalized to obtain the G/G_0 signal.

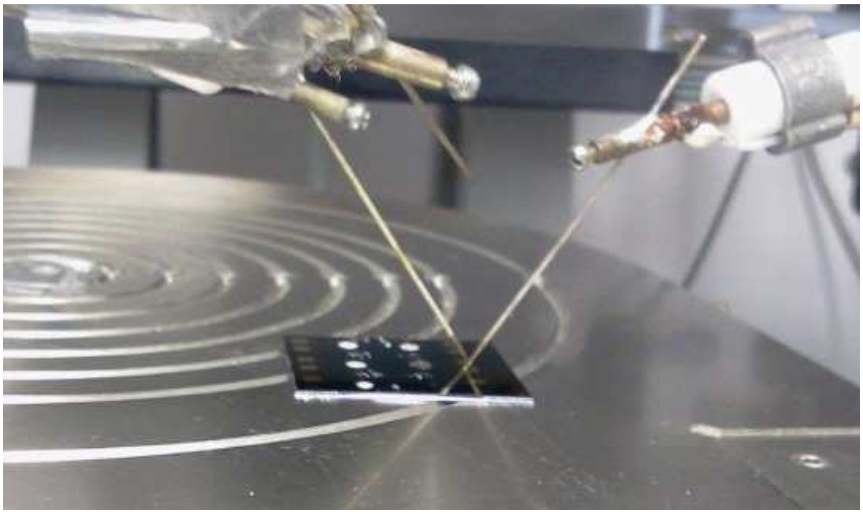

Figure III.7 Device during testing

The sensor element was also viewed an optical microscope to confirm the presence of cells (Figure III.8). A concentration of 10,000 cells/µL consistently covered the sensor element with 20-30 cells. Multiple MCF-7 and MCF-10A samples were tested at each session, along with blank PBS and DI water samples.

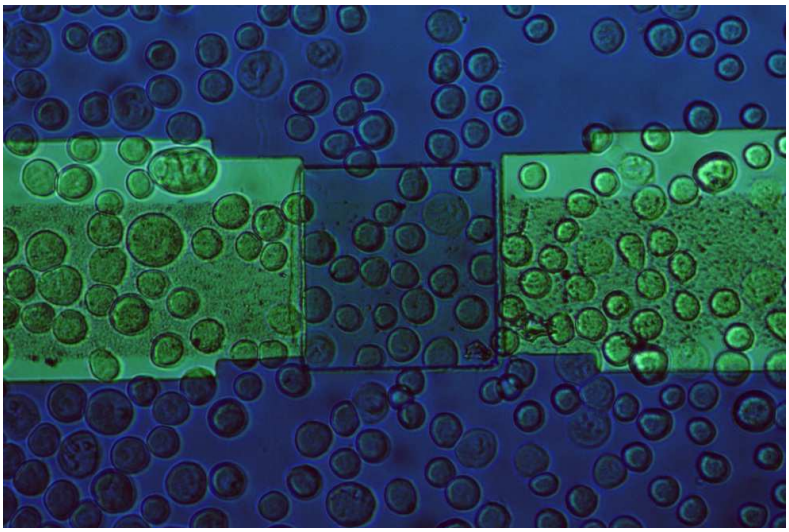

Figure III.8 MCF-10A cells after being pipetted onto the sensor

IV. RESULTS AND DISCUSSION

A. Sensor Development

Sensor reliability is one of the primary barriers to mainline adoption of carbon nanotube biosensors. The first tests carried out using these devices were done in a similar manner to the protocols reported for much smaller biosensors. The sensor, dry and exposed to air, was probed and a 100 mV bias applied for 300 seconds. At 30 seconds, a sample of cells suspended in PBS was pipetted onto the device. Wetting the sensor with the buffer attenuated the current as expected. Unfortunately, this attenuation was very inconsistent from device to device. About one in ten devices also underwent a steady increase, then decrease in current. Thus any signals arising due to specific binding were masked by the sudden and drastic change in the sensor environment. Many repetitions failed to generate a discernible pattern, or a characteristic difference between the specific and nonspecific binding signatures.

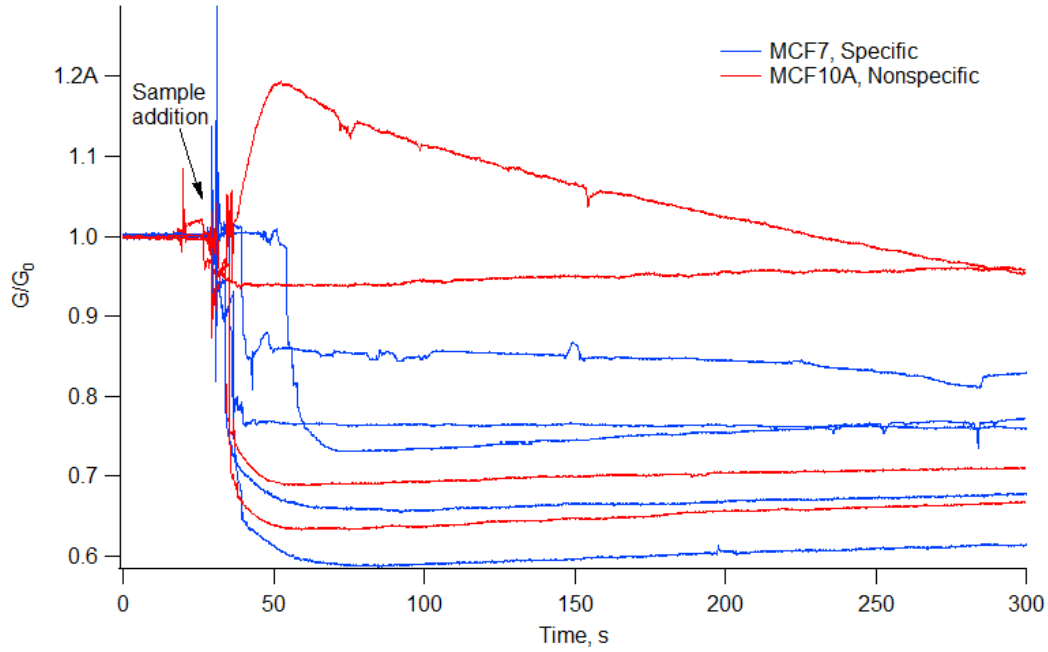

Figure IV.1 Inconsistent readings upon sample introduction to dry sensors

Placing a PBS droplet on the device before or after applying the V_{DS} bias removed the initial-hydration current attenuation from the sample interaction signal. However, noisy and anomalous readings persisted upon addition of the cell samples. Reproducible signals remained impossible to obtain.

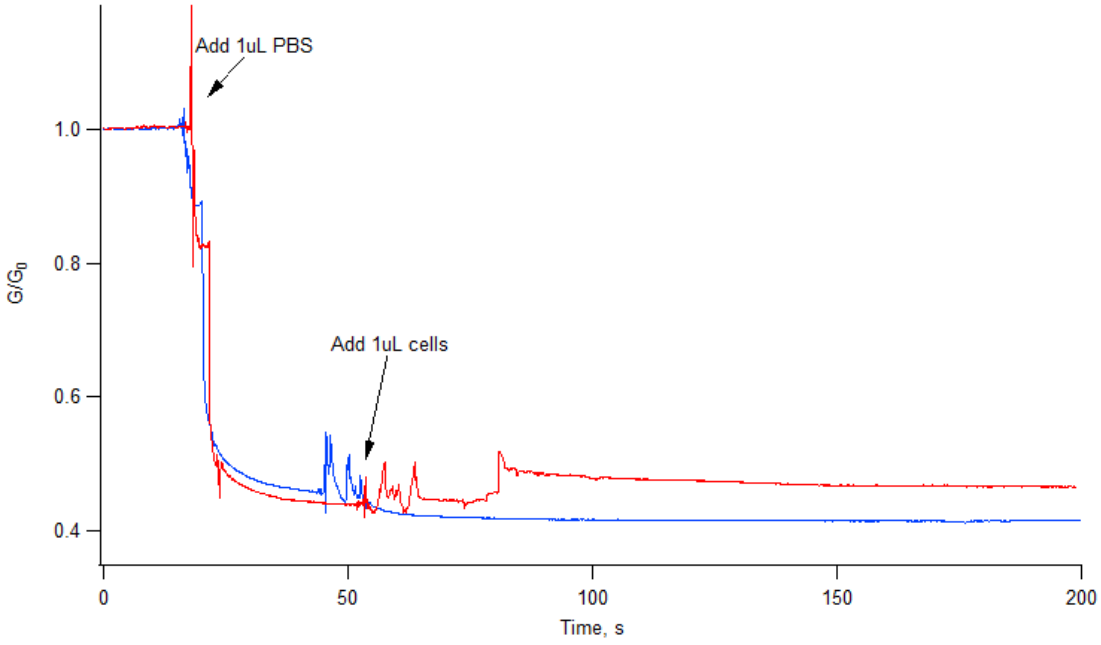

Figure IV.2 Noise associated with sample testing persists when loading after a PBS droplet

Attempting to avoid the noise associated with the liquid sample introduction, a study was conducted over extended time intervals. Cell samples at a concentration of 10,000 cells/μL were added to the devices and placed incubated at 37°C. A current measurement was taken at 2 hours, 4 hours and 8 hours. Then the cells were fixed in methanol, incubated in PBS overnight, and another reading was taken the next day. There was no statistically significant difference between the MCF7 and MCF-10A samples. But the pattern which emerged saw the current in all devices increase slightly up to the 4 hour time point, then decrease at the 8 hour and post fixation time points to below the initial value. This indicated that incubation in aqueous solutions alone was altering the nanotube conductance.

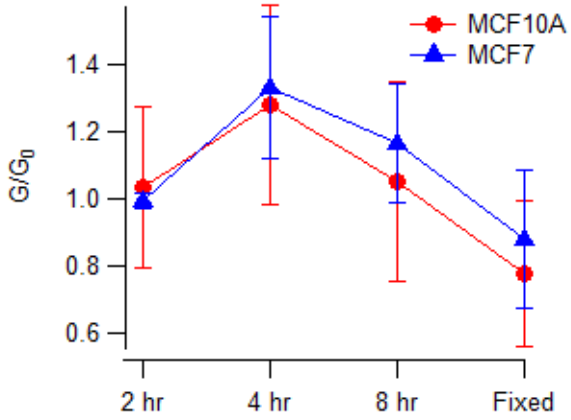

Figure IV.3 Conductance evolution in devices during incubation in PBS-cell suspension. G_0 was the conductance of the device prior to addition of the cells.

Tests on bare, unfunctionalized carbon nanotube devices revealed that extended incubation in water resulted in decreased conductivity of the device. Furthermore, device conductance gradually increased as they were exposed to air following fabrication. This effect was reversed by storing the fabricated sensors in a vacuum chamber.

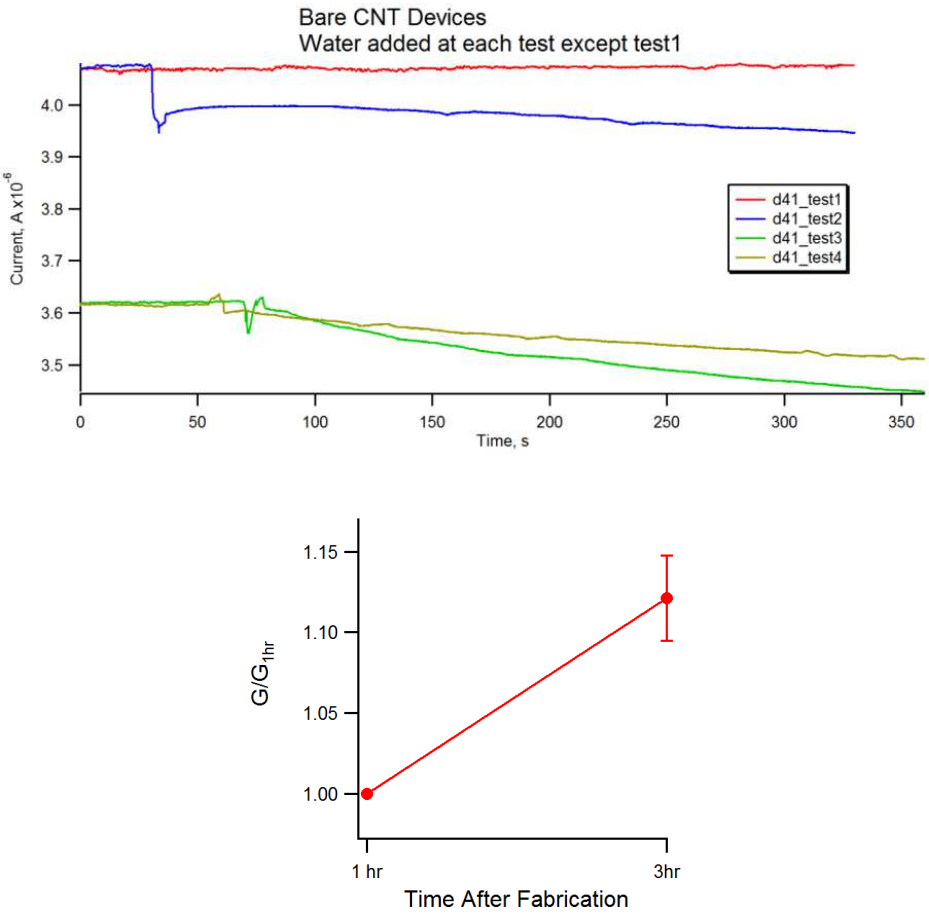

Figure IV.4 Device conductance changes for air and water exposure.

Altogether these findings indicate that gas molecules were reversibly doping the carbon nanotubes; Carbon nanotubes can be extremely sensitive to these effects [64]. The effect accumulated as they were exposed to air, and was reversed for vacuum and liquid environments. When in these environments, high concentrations of gas molecules in the vicinity of the nanotubes would either be drawn out into the vacuum or dissolved into the liquid. It was the reversing of the doping effects which lead to erratic behavior of the sensor.

Table IV.1 Effects on carbon nanotube conductance

Environment	Effect on Device current
Aqueous: Water/PBS	Decrease
Air	Increase
Vacuum	Decrease

Therefore, a fabrication and functionalization protocol was developed (as described in Section III) which eliminates long term exposure and minimizes the nanotubes total exposure to air as soon as the cleanroom fabrication steps are complete. The photolithography processing should result in consistent levels of CNT doping among sensors upon fabrication completion, so it was assumed that t=0 for air exposure at the moment the last photolithography step is complete.

Devices constructed with this minimal air exposure method produced much more consistent responses to blank PBS solutions for one hour (Figure IV.5). Additional PBS droplets had to be added to prevent the devices from drying out during the test. The humid chamber could not interface with the probe station so the devices were exposed to the dry room air. Bare and functionalized devices both exhibited similar curve shapes, a sharp drop in current followed by gradual recovery. However the functionalized device current gradually declined over the interval unlike the bare devices.

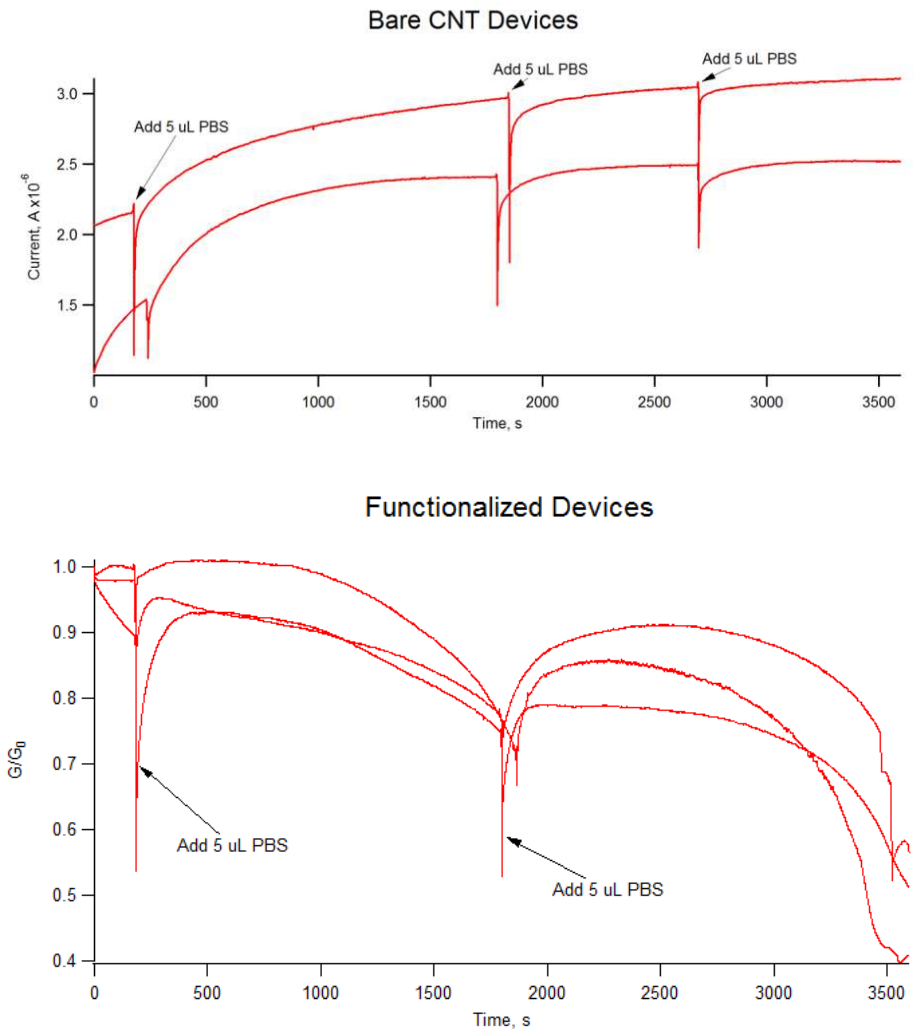

Figure IV.5 Consistent response to PBS addition for bare and functionalized devices

Consistent performing devices provided a stable platform to investigate the specific binding signature, although one small issue remains unresolved. When the bias is applied, some device currents drift upwards, some downwards, and some are steady. All three examples are shown in Figure IV.5 (b). It is unclear what effect, if any, this has on device sensitivity.

B. Specific Signature Identification

Elimination of noise due to gaseous doping enabled clear identification of the specific vs. nonspecific binding signatures. There was still variation during the first approximately 3 seconds of testing, but the devices soon reached a steady state value. For this reason the signals were normalized to the steady state value rather than the initial value. 9 devices were tested, 4 MCF-7, 4 MCF-10A, and 1 PBS control. The MCF-10A signals all had the characteristic shape for plain PBS addition as established previously. The PBS control reproduced this shape as well.

For the MCF-7 samples, 3 of the 4 exhibited an inverse shape while 1 had the nonspecific shape.

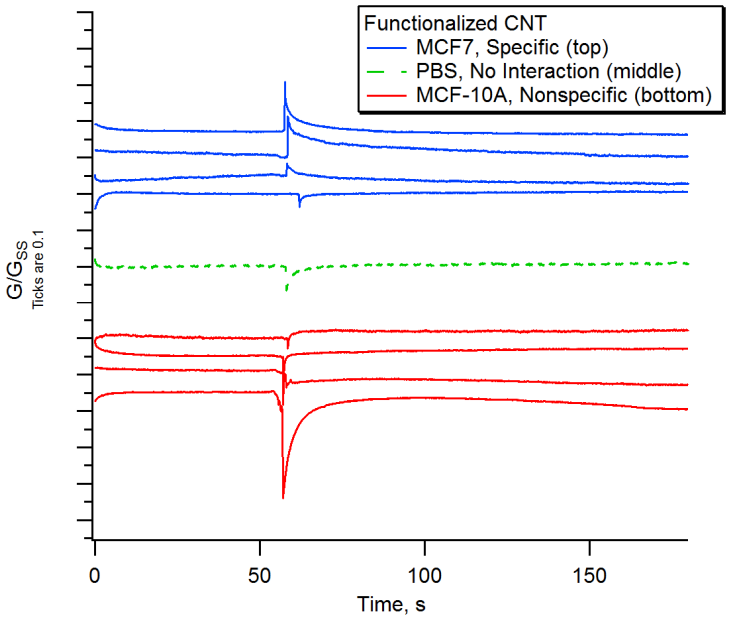

Figure IV.6 Specific vs. nonspecific cellular recognition signals. Signals are normalized to their steady state value before sample addition. They are plotted spaced apart for clarity.

To determine the statistical significance of this result, the average slope of the 0.4 seconds immediately following the prominent inflection point was calculated for each signal. Both data sets were determined to be random and of equal variance (appendix), therefore a two-sample t-test was used.

Table IV.2 *t*-test results

	MCF-7	**MCF10-A**
Calculated Slopes	-0.1469	0.162
	-0.0668	0.238
	-0.0601	0.0726
	0.0395	0.0291
Average	-0.0586	0.1254
Std. Deviation	0.0764	0.0932
***t* statistic**	-3.05326	
Critical	+/-2.47015	
***p* value**	0.02352	

The p value of $0.024 < 0.05$ denotes that there is a significant difference between the sampled MCF-7 signals and MCF-10A signals. This shows that the sensor is capable of differentiating between two cell populations which are very similar except for their surface markers, the first such accomplishment for a carbon nanotube-entangled network electrical sensor. Surface marker mediated cellular identification is the basis for detection of circulating tumor cells moving forward.

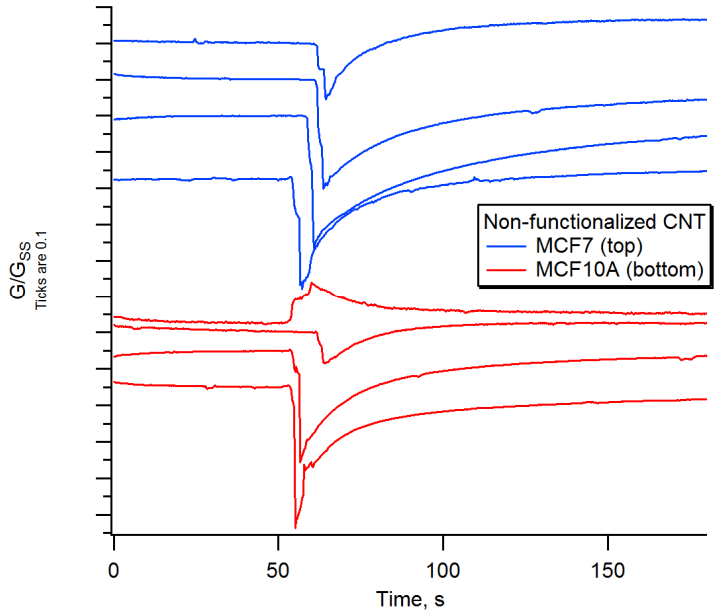

Figure IV.7 MCF-7 and MCF-10A cells placed on sensors with non-functionalized CNT films. Curves were similar to those for nonspecific interaction with the functionalized sensors and there was no statistical difference between the two cell types.

To test whether the different readings were due to a difference between the two cell types, rather than the presence or absence of EpCAM, the same tests were done using non-functionalized nanotube films (Figure IV.7). With one exception, the characteristic nonspecific signal was recorded all tests, and there was not a statistical difference between the two cell types when comparing the slope following the signal maximum or minimum, as was done for the functionalized sensor tests (Appendix).

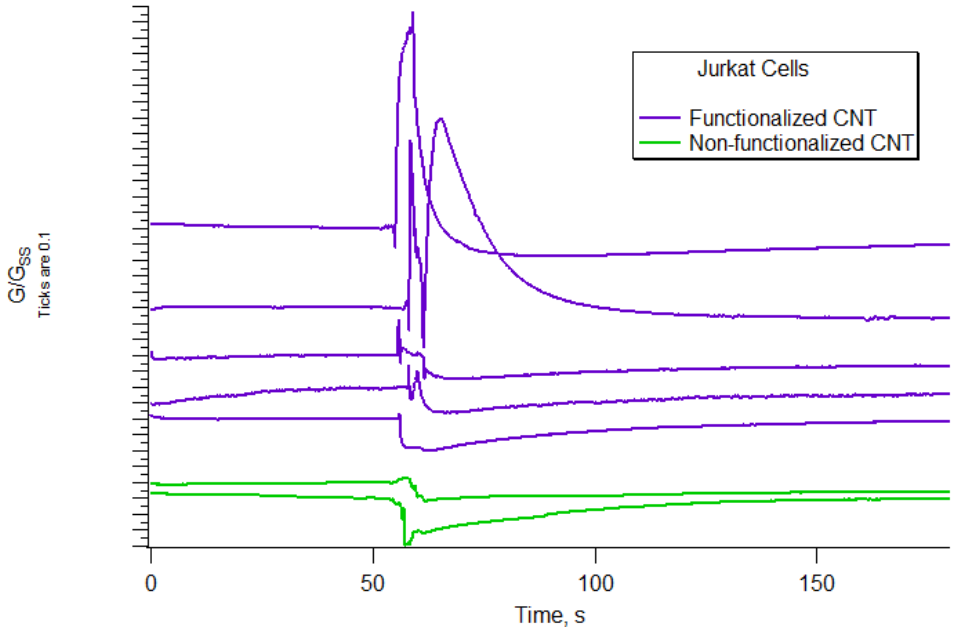

Figure IV.8 Jurkat E6-1 cell testing with functionalized and non-functionalized devices.

Additional controls were done with the Jurkat E6-1 cells, CD4+ lymphoblasts. This cell line was selected because it certainly does not express EpCAM since it is not an epithelial cell (MCF-10A may still express very low levels of EpCAM). Tests with the Jurkats were inconclusive however. With the functionalized sensors, fluctuating signals were observed following sample addition but non-functionalized sensors produced more typical nonspecific signals.

C. Interpretation

1. Epithelial Cell Lines

The MCF7 and MCF10A cell lines, like most mammalian non-excitable cells have a negative resting potential. The potential is maintained by active transport of ions, mainly sodium and potassium, across the membrane in order to facilitate transport of other chemical species. MCF7 potential was reported to vary from -58.6 mV to -2.7 mV with the cell cycle[65]. MCF10A membrane potential is estimated to be about -10 mV [66] but a similar report correlated to the cell cycle is not available.

As MCF7 cells reached the sensor and EpCAM units bound to the anti-EpCAM of the sensor, the sharp increase in conductance suggested an initial gating effect where the negatively charged MCF7s switched on the p-type semiconducting nanotubes. The sensor current then began to gradually return to near its initial value, either due to a loss of charge by the cell or current leakage through the antibody-PASE linkage binding the cell to the antibodies. The cell cycle dependent membrane potential of the MCF7 may also have caused the signal to vary among tests based on the net membrane potential of the 20-30 cells interfacing with the device for a given experiment.

Introduction of MCF10A to the device produced an opposite shaped curve, of the same shape as for blank PBS addition, supporting the hypothesis that specific interaction is required for the cell to affect the device. The cause of the shape of the curve produced by the nonspecific MCF10A samples and blank PBS with no interaction is uncertain. Perhaps it was due in part to the agitation of the fluid upon pipetting.

A thorough comparison of the membrane potentials of the MCF7 and MCF10A lines would strongly confirm these findings, if the two line are found to have equivalent membrane potentials. It is difficult to assume so because tumorigenisis and cell cycle deregulation are often closely linked [67], [68] and if the MCF7 cell cycle is sufficiently deviated from the MCF10A, it could result in the two cell populations having different membrane potential distributions.

The lack of a statistical difference between the two cell types in the control tests with the non-functionalized sensors does show that the results for functionalized sensors are not solely due to a difference in membrane potentials or other physical properties of the two cell lines.

2. Jurkat Cell Line

Testing with the Jurkat cells produced fluctuating signals where the characteristic nonspecific signal was expected. A possible explanation for this is that the Jurkat cells were responding to the non-human (mouse) IgG of the functionalized devices. This would initiate calcium-mediated potassium channel activation [69] and the flux of ions could be responsible for the signals observed. Additional tests would be needed to determine whether this effect is indeed occurring. It will also be an important consideration moving forward, to neutralize any immune response to the device antibodies if present, because patient samples are likely to contain leukocytes.

V. CONCLUSIONS

A. Summary

This study shows, for the first time, sensing of cellular EpCAM by a thin film carbon nanotube device. The sensing is performed entirely on a simple two terminal device with no moving parts. Such simplicity would enable this type of device to readily be integrated with other micro/nano components for biotechnology. It is possible to envision these types of sensors in many applications: Remote areas or those without high-tech infrastructure, home use for patients who need to regularly monitor CTC counts or other levels, and even perhaps in implantable devices, wirelessly relaying real time data to physicians and care providers.

Development of the sensor throughout this study encountered and overcame many pitfalls, most notably the gas adsorption and desorption effects. The steps needed to control these errors were very simple. Minimizing device exposure to air and keeping the device constantly hydrated from the end of the biofunctionalization process to the initiation of testing transformed erratic unpredictable sensors into reliably performing ones. Further investigation is sure to find other ways to remove environmental disturbances and improve the device sensing capability

Identifying cells by their membrane potential and electrical properties could potentially push label-free detection inside the cell. Binding of cell surface proteins typically initiates signaling cascades, phosphorylating and cleaving molecules inside the cell. If these events could be transduced through a bound antibody-carbon nanotube array, it would give great insight into the oft shrouded inner workings of the cell.

B. Future Work

In order to focus on the specific binding signature, experiments were carried out in near ideal conditions. Sensor surfaces were completely covered by both the test and control cell lines. All tests were done with the cells suspended in PBS, with no other proteins in solution that might compete for binding sites or otherwise alter the experiment. Now that the specific cellular binding signature has been recorded, work can be done to improve the signal and detect the cells under more physiological conditions, alongside nonspecific cells and free proteins.

To move this technology forward, aspects of the device performance such as the short initial drift in current, and interaction with leukocytes remain to be characterized. Improvements can also be made to the device, including additional nanotube purification steps to remove amorphous carbon and carbon nanoparticles [70], [71], annealing to lower the metal contact resistance and desorb interfering molecules from the nanotube sidewalls [72]. Sensors may also be cleaned with acid for re-use [58] which would be a good test for reproducibility and to further isolate and characterize the specific signal.

There are many exciting applications for this technology in the future, both near and far. Continued development is sure to uncover more challenges, insights and opportunities.

REFERENCES CITED

[1] "FASTSTATS - Leading Causes of Death." http://www.cdc.gov/nchs/fastats/lcod.htm/

[2] M. C. Miller, G. V. Doyle, and L. W. M. M. Terstappen, "Significance of Circulating Tumor Cells Detected by the CellSearch System in Patients with Metastatic Breast Colorectal and Prostate Cancer.," *Journal of oncology*, vol. 2010, p. 617421, Jan. 2010.

[3] T. R. Ashworth, "A case of cancer in which cells similar to those in the tumours were seen in the blood after death," *Australian Medical Journal*, vol. 14, pp. 146–147, 1869.

[4] K. Pachmann, O. Camara, A. Kavallaris, U. Schneider, S. Schünemann, and K. Höffken, "Quantification of the response of circulating epithelial cells to neodadjuvant treatment for breast cancer: a new tool for therapy monitoring.," *Breast cancer research : BCR*, vol. 7, no. 6, pp. R975-9, Jan. 2005.

[5] H. Lee, T.-J. Yoon, J.-L. Figueiredo, F. K. Swirski, and R. Weissleder, "Rapid detection and profiling of cancer cells in fine-needle aspirates.," *Proceedings of the National Academy of Sciences of the United States of America*, vol. 106, no. 30, pp. 12459-64, Jul. 2009.

[6] D. F. Hayes and J. Smerage, "Is there a role for circulating tumor cells in the management of breast cancer?," *Clinical cancer research : an official journal of the American Association for Cancer Research*, vol. 14, no. 12, pp. 3646-50, Jun. 2008.

[7] Z. Panteleakou et al., "Detection of circulating tumor cells in prostate cancer patients: methodological pitfalls and clinical relevance.," *Molecular medicine (Cambridge, Mass.)*, vol. 15, no. 3–4, pp. 101-14, 2009.

[8] S. Meng et al., "HER-2 gene amplification can be acquired as breast cancer progresses.," *Proceedings of the National Academy of Sciences of the United States of America*, vol. 101, no. 25, pp. 9393-8, Jun. 2004.

[9] R. a Ghossein and S. Bhattacharya, "Molecular detection and characterisation of circulating tumour cells and micrometastases in solid tumours.," *European journal of cancer (Oxford, England : 1990)*, vol. 36, no. 13 Spec No, pp. 1681-94, Aug. 2000.

[10] "FDA Clears Cellsearch(TM) Circulating Tumor Cell Test for Monitoring Metastatic Prostate Cancer Patients," *PR Newswire*, 2008. [Online]. Available: http://www.prnewswire.com/news-releases/fda-clears-cellsearchtm-circulating-tumor-cell-test-for-monitoring-metastatic-prostate-cancer-patients-57318572.html. [Accessed: 06-Apr-2012].

[11] L. W. M. M. Terstappen, G. C. Rao, J. W. Uhr, E. V. Racila, and P. A. Liberti, "Methods and reagents for the rapid and efficient isolation of circulating cancer cells," U.S. Patent 7,332,2882008.

[12] Veridex LLC, *CellSearch(R) Video*. 2012.

[13] W. J. Allard et al., "Tumor cells circulate in the peripheral blood of all major carcinomas but not in healthy subjects or patients with nonmalignant diseases.," *Clinical cancer research : an official journal of the American Association for Cancer Research*, vol. 10, no. 20, pp. 6897-904, Oct. 2004.

[14] "New Veridex Alliance Drives Study Of Circulating Tumor Cells In Men With Metastatic Prostate Cancer," *PR Newswire*, 2012. [Online]. Available: http://www.prnewswire.com/news-releases/new-veridex-alliance-drives-study-of-circulating-tumor-cells-in-men-with-metastatic-prostate-cancer-148519765.html. [Accessed: 06-Apr-2012].

[15] J. M. Walker and R. Rapley, *Molecular Biomethods Handbook*, 2nd ed. 2008.

[16] P. a Baeuerle and O. Gires, "EpCAM (CD326) finding its role in cancer.," *British journal of cancer*, vol. 96, no. 3, pp. 417-23, Feb. 2007.

[17] M. Herlyn, Z. Steplewski, D. Herlyn, and H. Koprowski, "Colorectal carcinoma-specific antigen: detection by means of monoclonal antibodies.," *Proceedings of the National Academy of Sciences of the United States of America*, vol. 76, no. 3, pp. 1438-42, Mar. 1979.

[18] M. Balzar, M. J. Winter, C. J. de Boer, and S. V. Litvinov, "The biology of the 17-1A antigen (Ep-CAM).," *Journal of molecular medicine (Berlin, Germany)*, vol. 77, no. 10, pp. 699-712, Oct. 1999.

[19] S. Sleijfer, J.-W. Gratama, A. M. Sieuwerts, J. Kraan, J. W. M. Martens, and J. a Foekens, "Circulating tumour cell detection on its way to routine diagnostic implementation?," *European journal of cancer (Oxford, England : 1990)*, vol. 43, no. 18, pp. 2645-50, Dec. 2007.

[20] P. Paterlini-Brechot and N. L. Benali, “Circulating tumor cells (CTC) detection: clinical impact and future directions.,” *Cancer letters*, vol. 253, no. 2, pp. 180-204, Aug. 2007.

[21] S. Nagrath et al., “Isolation of rare circulating tumour cells in cancer patients by microchip technology.,” *Nature*, vol. 450, no. 7173, pp. 1235-9, Dec. 2007.

[22] B. Panchapakesan et al., “Micro- and nanotechnology approaches for capturing circulating tumor cells,” *Cancer Nanotechnology*, vol. 1, no. 1–6, pp. 3-11, Oct. 2010.

[23] J. H. Myung, K. a Gajjar, J. Saric, D. T. Eddington, and S. Hong, “Dendrimer-Mediated Multivalent Binding for the Enhanced Capture of Tumor Cells.,” *Angewandte Chemie (International ed. in English)*, pp. 1-5, Oct. 2011.

[24] F. Fachin, G. D. Chen, M. Toner, and B. L. Wardle, “Integration of Bulk Nanoporous Elements in Microfluidic Devices With Application to Biomedical Diagnostics,” *Journal of Microelectromechanical Systems*, vol. 20, no. 6, pp. 1428-1438, Dec. 2011.

[25] G. D. Chen, F. Fachin, M. Fernandez-Suarez, B. L. Wardle, and M. Toner, “Nanoporous elements in microfluidics for multiscale manipulation of bioparticles.,” *Small (Weinheim an der Bergstrasse, Germany)*, vol. 7, no. 8, pp. 1061-7, Apr. 2011.

[26] V. Parichehreh and P. Sethu, “Inertial lift enhanced phase partitioning for continuous microfluidic surface energy based sorting of particles.,” *Lab on a chip*, vol. 12, no. 7, pp. 1296-301, Apr. 2012.

[27] V. Moy, E.-ludwig Florin, and H. Gaub, “Intermolecular forces and energies between ligands and receptors,” *Science*, vol. 266, no. 5183, pp. 257-259, Oct. 1994.

[28] J. Fritz et al., “Translating biomolecular recognition into nanomechanics,” *Science*, vol. 288, no. 5464, pp. 316-318, 2000.

[29] G. Wu, R. H. Datar, K. M. Hansen, T. Thundat, R. J. Cote, and A. Majumdar, “Bioassay of prostate-specific antigen (PSA) using microcantilevers.,” *Nature biotechnology*, vol. 19, no. 9, pp. 856-60, Sep. 2001.

[30] G. Wu et al., “Origin of nanomechanical cantilever motion generated from biomolecular interactions.,” *Proceedings of the National Academy of Sciences of the United States of America*, vol. 98, no. 4, pp. 1560-4, Feb. 2001.

[31] M. Yue et al., “A 2-D Microcantilever Array for Multiplexed Biomolecular Analysis,” *Journal of Microelectromechanical Systems*, vol. 13, no. 2, pp. 290-299, Apr. 2004.

[32] Y. Ohno, K. Maehashi, K. Inoue, and K. Matsumoto, “Label-Free Aptamer-Based Immunoglobulin Sensors Using Graphene Field-Effect Transistors,” *Japanese Journal of Applied Physics*, vol. 50, no. 7, p. 070120, Jul. 2011.

[33] S. Iijima, “Helical microtubules of graphitic carbon,” *Nature*, vol. 354, no. 6348, pp. 56-58, Nov. 1991.

[34] S. Iijima and T. Ichihashi, “Single-shell carbon nanotubes of 1-nm diameter,” *Nature*, vol. 363, no. 6430, pp. 603-605, 1993.

[35] R. H. Baughman, A. A. Zakhidov, and W. A. de Heer, “Carbon nanotubes--the route toward applications.,” *Science (New York, N.Y.)*, vol. 297, no. 5582, pp. 787-92, Aug. 2002.

[36] M. Glerup, V. Krstic, C. Ewels, M. Holzinger, and G. Van Lier, “Doping of Carbon Nanotubes,” in *Doped Nanomaterials and Nanodevices*, W. Chen, Ed. American Scientific Publishers, 2010.

[37] Y. Yoon and J. Guo, “Analysis of Strain Effects in Ballistic Carbon Nanotube FETs,” *IEEE Transactions on Electron Devices*, vol. 54, no. 6, pp. 1280-1287, Jun. 2007.

[38] F. Balavoine, P. Schultz, C. Richard, V. Mallouh, T. W. Ebbesen, and C. Mioskowski, “Helical Crystallization of Proteins on Carbon Nanotubes: A First Step towards the Development of New Biosensors,” *Angewandte Chemie International Edition*, vol. 38, no. 13–14, pp. 1912-1915, Jul. 1999.

[39] R. J. Chen, Y. Zhang, D. Wang, and H. Dai, “Noncovalent Sidewall Functionalization of Single-Walled Carbon Nanotubes for Protein Immobilization,” *Journal of the American Chemical Society*, vol. 123, no. 16, pp. 3838-3839, 2001.

[40] R. A. V. Gallardo, “BIOSENSORS BASED ON CARBON NANOTUBE FIELD EFFECT TRANSISTORS (CNTFETs) FOR DETECTING PATHOGENIC MICROORGANISMS,” UNIVERSITAT ROVIRA I VIRGILI, 2010.

[41] T. Kurkina, A. Vlandas, A. Ahmad, K. Kern, and K. Balasubramanian, “Label-free detection of few copies of DNA with carbon nanotube impedance biosensors.,” *Angewandte Chemie (International ed. in English)*, vol. 50, no. 16, pp. 3710-4, Apr. 2011.

[42] H. Cai, X. Cao, Y. Jiang, P. He, and Y. Fang, "Carbon nanotube-enhanced electrochemical DNA biosensor for DNA hybridization detection.," *Analytical and bioanalytical chemistry*, vol. 375, no. 2, pp. 287-93, Jan. 2003.

[43] C. B. Jacobs, M. J. Peairs, and B. J. Venton, "Review: Carbon nanotube based electrochemical sensors for biomolecules.," *Analytica chimica acta*, vol. 662, no. 2, pp. 105-27, Mar. 2010.

[44] Q. Cao and J. A. Rogers, "Ultrathin Films of Single-Walled Carbon Nanotubes for Electronics and Sensors: A Review of Fundamental and Applied Aspects," *Advanced Materials*, vol. 21, no. 1, pp. 29-53, Jan. 2009.

[45] B. L. Allen, P. D. Kichambare, and A. Star, "Carbon Nanotube Field-Effect-Transistor-Based Biosensors," *Advanced Materials*, vol. 19, no. 11, pp. 1439-1451, Jun. 2007.

[46] D. Lee and T. Cui, "Low-cost, transparent, and flexible single-walled carbon nanotube nanocomposite based ion-sensitive field-effect transistors for pH/glucose sensing.," *Biosensors & bioelectronics*, vol. 25, no. 10, pp. 2259-64, Jun. 2010.

[47] S. . Wang, Q. Zhang, R. Wang, and S. . Yoon, "A novel multi-walled carbon nanotube-based biosensor for glucose detection," *Biochemical and Biophysical Research Communications*, vol. 311, no. 3, pp. 572-576, Nov. 2003.

[48] D. Lee and T. Cui, "Carbon nanotube thin film pH electrode for potentiometric enzymatic acetylcholine biosensing," *Microelectronic Engineering*, vol. 93, pp. 39-42, May 2012.

[49] S. Mao, G. Lu, K. Yu, and J. Chen, "Specific biosensing using carbon nanotubes functionalized with gold nanoparticle–antibody conjugates," *Carbon*, vol. 48, no. 2, pp. 479-486, Feb. 2010.

[50] R. J. Chen et al., "Noncovalent functionalization of carbon nanotubes for highly specific electronic biosensors," *Proceedings of the National Academy of Sciences of the United States of America*, vol. 100, no. 9, pp. 4984-4989, 2003.

[51] A. Palaniappan et al., "Aligned carbon nanotubes on quartz substrate for liquid gated biosensing.," *Biosensors & bioelectronics*, vol. 25, no. 8, pp. 1989-93, Apr. 2010.

[52] J. P. Kim, B. Y. Lee, J. Lee, S. Hong, and S. J. Sim, "Enhancement of sensitivity and specificity by surface modification of carbon nanotubes in diagnosis of prostate cancer based on carbon nanotube field effect transistors.," *Biosensors & bioelectronics*, vol. 24, no. 11, pp. 3372-8, Jul. 2009.

[53] J. P. Kim, B. Y. Lee, S. Hong, and S. J. Sim, “Ultrasensitive carbon nanotube-based biosensors using antibody-binding fragments.,” *Analytical biochemistry*, vol. 381, no. 2, pp. 193-8, Oct. 2008.

[54] N. Shao, E. Wickstrom, and B. Panchapakesan, “Nanotube-antibody biosensor arrays for the detection of circulating breast cancer cells.,” *Nanotechnology*, vol. 19, no. 46, p. 465101, Nov. 2008.

[55] A. Zani, S. Laschi, M. Mascini, and G. Marrazza, “A New Electrochemical Multiplexed Assay for PSA Cancer Marker Detection,” *Electroanalysis*, vol. 23, no. 1, pp. 91-99, Jan. 2011.

[56] R. S. Gaster et al., “Matrix-insensitive protein assays push the limits of biosensors in medicine.,” *Nature medicine*, vol. 15, no. 11, pp. 1327-32, Nov. 2009.

[57] H. R. Byon and H. C. Choi, “Network single-walled carbon nanotube-field effect transistors (SWNT-FETs) with increased Schottky contact area for highly sensitive biosensor applications.,” *Journal of the American Chemical Society*, vol. 128, no. 7, pp. 2188-9, Feb. 2006.

[58] E. D. Minot, A. M. Janssens, I. Heller, H. a. Heering, C. Dekker, and S. G. Lemay, “Carbon nanotube biosensors: The critical role of the reference electrode,” *Applied Physics Letters*, vol. 91, no. 9, p. 093507, 2007.

[59] I. Heller, A. M. Janssens, J. Männik, E. D. Minot, S. G. Lemay, and C. Dekker, “Identifying the mechanism of biosensing with carbon nanotube transistors.,” *Nano letters*, vol. 8, no. 2, pp. 591-5, Mar. 2008.

[60] J. J. Gooding, “Nanostructuring electrodes with carbon nanotubes: A review on electrochemistry and applications for sensing,” *Electrochimica Acta*, vol. 50, no. 15, pp. 3049-3060, 2005.

[61] C. Li et al., “Complementary detection of prostate-specific antigen using In2O3 nanowires and carbon nanotubes.,” *Journal of the American Chemical Society*, vol. 127, no. 36, pp. 12484-5, Sep. 2005.

[62] W. a Osta et al., “EpCAM is overexpressed in breast cancer and is a potential target for breast cancer gene therapy.,” *Cancer research*, vol. 64, no. 16, pp. 5818-24, Aug. 2004.

[63] Z. Wu et al., “Transparent, conductive carbon nanotube films.,” *Science (New York, N.Y.)*, vol. 305, no. 5688, pp. 1273-6, Aug. 2004.

[64] P. G. Collins, “Extreme Oxygen Sensitivity of Electronic Properties of Carbon Nanotubes,” *Science*, vol. 287, no. 5459, pp. 1801-1804, Mar. 2000.

[65] W. F. Wonderlin, K. A. Woodfork, and J. S. Strobl, “Changes in membrane potential during the progression of MCF-7 human mammary tumor cells through the cell cycle.,” *Journal of cellular physiology*, vol. 165, no. 1, pp. 177-85, Oct. 1995.

[66] P. Sun, F. O. Laforge, T. P. Abeyweera, S. a Rotenberg, J. Carpino, and M. V. Mirkin, “Nanoelectrochemistry of mammalian cells.,” *Proceedings of the National Academy of Sciences of the United States of America*, vol. 105, no. 2, pp. 443-8, Jan. 2008.

[67] Z. Yu and R. G. Pestell, “Small Non-coding RNAs Govern Mammary Gland Tumorigenesis.,” *Journal of mammary gland biology and neoplasia*, vol. 17, no. 1, pp. 59-64, Mar. 2012.

[68] R. D. Coletta, P. Jedlicka, A. Gutierrez-Hartmann, and H. L. Ford, “Transcriptional control of the cell cycle in mammary gland development and tumorigenesis.,” *Journal of mammary gland biology and neoplasia*, vol. 9, no. 1, pp. 39-53, Jan. 2004.

[69] C. M. Fanger et al., “Calcium-activated potassium channels sustain calcium signaling in T lymphocytes. Selective blockers and manipulated channel expression levels.,” *The Journal of biological chemistry*, vol. 276, no. 15, pp. 12249-56, Apr. 2001.

[70] H. Hu et al., “Influence of the zeta potential on the dispersability and purification of single-walled carbon nanotubes.,” *The journal of physical chemistry. B*, vol. 109, no. 23, pp. 11520-4, Jun. 2005.

[71] A. Yu, E. Bekyarova, M. E. Itkis, D. Fakhrutdinov, R. Webster, and R. C. Haddon, “Application of centrifugation to the large-scale purification of electric arc-produced single-walled carbon nanotubes.,” *Journal of the American Chemical Society*, vol. 128, no. 30, pp. 9902-8, Aug. 2006.

[72] Q. Zhang, P. Vichchulada, S. B. Shivareddy, and M. D. Lay, “Reducing electrical resistance in single-walled carbon nanotube networks: effect of the location of metal contacts and low-temperature annealing,” *Journal of Materials Science*, vol. 47, no. 7, pp. 3233-3240, Dec. 2011.

APPENDIX

CNT Film density

V_npnts= 273; V_numNaNs= 0; V_numINFs= 0; V_avg= 3.93407;

V_Sum= 1074; V_sdev= 3.22947; V_sem= 0.195456; V_rms= 5.08607;

V_adev= 2.49213; V_skew= 1.23362; V_kurt= 1.70445; V_minloc= 6;

V_maxloc= 216; V_min= 0; V_max= 17; V_minRowLoc= 6;

V_minColLoc= 0; V_maxRowLoc= 8; V_maxColLoc= 16; V_startRow= 0;

V_endRow= 272;

CNT Film Lorentzian fit (Figure III.3)

Fit converged properly

fit_MegaWAve_Hist= W_coef[0]+W_coef[1]/((x-W_coef[2])^2+W_coef[3])

W_coef={-0.27186,389.49,2.2585,8.8351}

V_chisq= 221.487;V_npnts= 100;V_numNaNs= 0;V_numINFs= 0;

V_startRow= 0;V_endRow= 99;

W_sigma={0.169,28.9,0.0781,0.769}

Coefficient values ± one standard deviation

y0 =-0.27186 ± 0.169

A =389.49 ± 28.9

x0 =2.2585 ± 0.0781

B =8.8351 ± 0.769

Statistical Analysis, Functionalized Sensors

Serial Randomness Test for root:wave3 (MCF7)

P>alpha so do not reject the hypothesis that the data are random.

Point	W_StatsSRTest.l	W_StatsSRTest.d	
0	N	4	
1	Runs Up	1	
2	Runs Down	0	
3	Unchanged	0	
4	Longest Run	1	
5	Longest Run Prob	0.903028	
6	Total Runs	1	
7	Prob	0.0833333	
8			

Serial Randomness Test for root:wave4 (MCF10A)

P>alpha so do not reject the hypothesis that the data are random.

Point	W_StatsSRTest.l	W_StatsSRTest.d	
0	N	4	
1	Runs Up	1	
2	Runs Down	1	
3	Unchanged	0	
4	Longest Run	1	
5	Longest Run Prob	0.903028	
6	Total Runs	2	
7	Prob	0.583333	
8			

F test for root:wave3 and root:wave4

F statistic inside the critical range => do not reject hypothesis of equal variances.

Point	W_StatsFTest.l	W_StatsFTest.d	
0	n1	4	
1	Mean1	-0.058575	
2	Stdv1	0.0763544	
3	degreesOfFreedom1	3	
4	n2	4	
5	Mean2	0.125425	
6	Stdv2	0.0932378	
7	degreesOfFreedom2	3	
8	F	0.670632	
9	lowCriticalValue	0.0647703	
10	highCriticalValue	15.4392	
11	P	0.750615	
12	Accept	1	
13			

T test for independent samples root:wave3 and root:wave4

Abs(t_statistic)>=Critical => there is significant difference between the populations

Point	W_StatsTTest.l	W_StatsTTest.d	
0	n1	4	
1	DF1	3	
2	avg1	-0.058575	
3	stdv1	0.0763544	
4	n2	4	
5	DF2	3	
6	avg2	0.125425	
7	stdv2	0.0932378	
8	t statistic	-3.05362	
9	P	0.0235184	
10	DFc	5.77551	
11	lowCritical	-2.47015	
12	highCritical	2.47015	
13	CI 1 Low	-0.119323	
14	CI 1 High	0.00217345	
15	CI 2 Low	0.0512439	
16	CI 2 High	0.199606	
17	Accept	0	
18			

Statistical Analysis, non-functionalized sensors

Data Sets

MCF10A	MCF7
0.0497192	0.0362276
0.0296412	0.00990511
0.00212742	0.0239869
-0.00961552	0.0442623

Serial Randomness Test for root:mcf10a_blank4slopes

P>alpha so do not reject the hypothesis that the data are random.

Point	W_StatsSRTest.l	W_StatsSRTest.d	
0	N	4	
1	Runs Up	0	
2	Runs Down	1	
3	Unchanged	0	
4	Longest Run	1	
5	Longest Run Prob	0.903028	
6	Total Runs	1	
7	Prob	0.0833333	
8			

Serial Randomness Test for root:mcf7_blank4slopes

P>alpha so do not reject the hypothesis that the data are random.

Point	W_StatsSRTest.l	W_StatsSRTest.d	
0	N	4	
1	Runs Up	1	
2	Runs Down	1	
3	Unchanged	0	
4	Longest Run	1	
5	Longest Run Prob	0.903028	
6	Total Runs	2	
7	Prob	0.583333	
8			

F test for root:mcf10a_blank4slopes and root:mcf7_blank4slopes

F statistic inside the critical range => do not reject hypothesis of equal variances.

Point	W_StatsFTest.l	W_StatsFTest.d	
0	n1	4	
1	Mean1	0.0179681	
2	Stdv1	0.0268091	
3	degreesOfFreedom1	3	
4	n2	4	
5	Mean2	0.0285955	
6	Stdv2	0.0149919	
7	degreesOfFreedom2	3	
8	F	3.19781	
9	lowCriticalValue	0.0647703	
10	highCriticalValue	15.4392	
11	P	0.365231	
12	Accept	1	
13			

T test for independent samples root:mcf10a_blank4slopes and root:mcf7_blank4slopes

Abs(t_statistic)<Critical => there is no significant difference between the populations

Point	W_StatsTTest.l	W_StatsTTest.d	
0	n1	4	
1	DF1	3	
2	avg1	0.0179681	
3	stdv1	0.0268091	
4	n2	4	
5	DF2	3	
6	avg2	0.0285955	
7	stdv2	0.0149919	
8	t_statistic	-0.691975	
9	P	0.521576	
10	DFc	4.70915	
11	lowCritical	-2.61908	
12	highCritical	2.61908	
13	pooledMean	0.0232818	
14	pooledMean	1.47419e-05	
15	CI_P_Low	0.0197923	
16	CI_P_High	0.0267713	
17	Accept	1	
18			

VITA

Benjamin C. King
131 W Collins Ct.
Louisville, KY 40214
bcking21@gmail.com
Tel:270-792-3441

I. Education

Master of Engineering in Bioengineering, August 2012
3.9/4.0 GPA JB Speed School of Engineering, University of Louisville, Louisville, KY
Thesis topic: Carbon Nanotube Biosensors for Detection of Biomarkers in Breast Cancer Cells,
Advisor: Dr. Balaji Panchapakesan, Small Systems Laboratory.

Bachelor of Science in Bioengineering , May 2009
3.6/4.0 GPA JB Speed School of Engineering, University of Louisville, Louisville, KY

Sr. Design Project: MRI Image Processing Algorithm for Non-Invasive Measurement of Transplant Kidney Function.

II. Experience

Graduate Research Assistant May 2009 – Present
Small Systems Laboratory, 221 Shumaker Research Building, University of Louisville (Louisville, KY)
Device Development Based on Carbon Nanotubes

- Detection of cell surface markers via carbon nanotube immunosensors.
- Network mechanics and alignment of carbon nanotubes using lateral force microscopy.
- Characterization of dimensional dependence of mechanical response to near infra-red light based on 1D, 2D and 3D carbon forms.

Quantitative carbon nanotube film measurements with AFM

- Synchronous electrical and force measurements
- Thickness and density measurements via topography histograms

Materials characterization

- Compare Raman scattering of 1D, 2D and 3D carbon forms, both isolated graphene and in polymer-graphene composites
- Temperature controlled analysis of Raman spectroscopy in graphene films, down to -140°C

Data processing and analysis

- Image correction, section and histogram analysis of AFM data, Igor Pro
- Fourier analysis and filtering of electrical signals, MATLAB
- Analysis of Variance in carbon nanotube mechanical response to AFM force, frequency and scan rate, Minitab

Research Assistant (Engineering Co-op) May 2008– May 2009
Center for Regulatory and Environmental Analytical Metabolomics (Louisville, KY)
Performed cell culture and wet lab work for metabolomic experiments
Carried out mass spectrometry analysis
Coded chemoinformatics programming

Process Engineering Co-op August 2007– December 2007
Boston Scientific Corporation (Spencer, IN)
Product testing in compliance with FDA regulations and good documentation practices
Updated and organized validation documents for multiple product lines
Created and submitted product build orders for testing

Professtional Affiliations and Awards

Dean's List: Spring 2006, Spring 2007, Summer 2007, Spring 2008, Fall 2008
Tau Beta Pi Engineering Honor Society, 2007-present
Biomedical Engineering Society, 2007-2008
Phi Eta Sigma Freshmen Honor Society, 2005-2006

III. Skills and Coursework

Materials Characterization: Scanning Electron Microscopy (SEM), AFM, Raman spectroscopy, Confocal and fluorescence microscopy
Micro/nano technology fabrication: Carbon nanotube film construction and patterning, photolithography, metal deposition, reactive ion etching.
Circuit design for instrumentation amplification
High level programming : MATLAB, Igor Pro, AutoCAD, Google SketchUp design and drafting

Select Courses:
Introduction to Micro/Nano Technology
Biosystems Controls
Introduction to Molecular Bioengineering
Random Processes and Estimation Theory
Anatomy and Physiology for Bioengineering
Differential Equations

IV. Journal Publications

James Loomis, **Ben King**, and Balaji Panchapakesan. "Layer Dependent Mechanical Responses of Graphene Composites to Near-Infrared Light." *Applied Physics Letters* 100 (7), (February 073108-073108-42012, Impact Factor 4.2

James Loomis, **Ben King**, Tom Burkhead, Peng Xu, Nathan Bessler, Eugene Terentjev, and Balaji Panchapakesan. "Graphene-nanoplatelet-based photomechanical actuators." *Nanotechnology* 23, no. 4 (February 3, 2012): 045501. http://www.ncbi.nlm.nih.gov/pubmed/22222415., Impact Factor: 3.65

Balaji Panchapakesan, Robert Caprara, Vanessa Velasco, James Loomis, **Ben King**, Peng Xu, Tom Burkhead, et al. "Micro- and nanotechnology approaches for capturing circulating

tumor cells." *Cancer Nanotechnology* 1, no. 1-6 (October 2010): 3-11. http://www.springerlink.com/index/10.1007/s12645-010-0007-z.

Shoaxin Lu, Samit Ahir, Vanessa Velasco, **Ben King**, Peng Xu, Eugene Terentjev, and Balaji Panchapakesan. "Photo-mechanical actuation of carbon nanotubes: mechanisms and applications in micro and nano-devices." *Journal of Micro - Nano Mechatronics* 5, no. 1 (2009): 29-41. http://dx.doi.org/10.1007/s12213-009-0021-6.

V. Conference Presentations

Benjamin C. King, Michael Clark, Thomas Burkhead, Palaniappan Sethu, Shesh Rai, Goetz Kloecker and Balaji Panchapakesan. "Electrical detection of specific versus nonspecific binding events in breast cancer cells." Oral presentation, *SPIE Photonics West*, San Diego, CA. August 12-16, 2012

Benjamin C. King, and Balaji Panchapakesan. "Nanoscale Plowing and Alignment of Individual Carbon Nanotubes from Randomly Oriented Networks Using Intertube Sliding in Liquid Atomic Force Microscopy." Oral Presentation*, Nanotechnology and Nanomedicine Symposium*, Sullivan University, Louisville, KY. September 24th, 2011

Benjamin King, Richard Higashi, and Teresa Fan. "Profiling Se-Containing Proteins in Cancer Cells by Laser Ablation – Inductively Coupled Plasma – Mass Spectrometery." Poster Presentation, *Undergraduate Research Symposium*, University of Louisville, Louisville KY. April 2009

Benjamin King, Teresa Cassel, Richard Higashi, and Teresa Fan. "Metabolomic Analysis of Selenium Anti-Cancer Agents for Chemopreventive Use." Poster Presentation, *Research!Louisville Symposium*, Louisville, KY. October 20th, 2008

Benjamin King, Palaniappan Sethu, and J. Christopher States. "Microfluidic Cell Array for Dosage and Time Response Studies." Poster Presentation, Biomedical Engineering Society Anuual Fall Meeting, St. Louis, MO. October 11th, 2008

Other Activities

Avid cyclist: ride for commuting as well as racing, mountain and road. Can also ride a unicycle.

Volleyball: play in local tournaments and regular pick-up games with fellow reseachers.

Music: play bass guitar solo for open mic nights or in ensembles with friends.